Journal of Thermal Analysis, Vol. 54 (1998) 741-752

SIZE DISTRIBUTION OF WATER DROPLETS IN BUTYL RUBBER
Application of DSC in thermoporosimetry

R. Neffati[1], *L. Apekis*[2] *and J. Rault*[1*]

[1]Physique des Solides, Université Paris-Sud, 91405 Orsay, France
[2]National Technical University of Athens, Zografan campus, 15773 Athens, Greece

(Received December 5, 1997)

Abstract

It is shown that for porous systems filled with a solvent, if the temperature domains of crystallization and melting of the solvent are well separated, DSC technique, combined with suitably chosen thermal cycles, provides crystallization and melting curves which are independent of a) the mass of the material, b) the thermal contact between DSC pan and material and c) the thermal conductivity of the material. This method called DSC fractionation is applied to butyl rubber containing small water nodules. Thermoporosimetry is then applied to get the size distribution of mesoscopic solvent droplets.

Keywords: butyl rubber, confinement, DSC, thermoporosimetry, water crystallization, water droplet

Introduction

Porous materials have a great technological importance. It is well known that in these materials the dynamic and thermodynamic properties of confined liquids are different from those of the bulk (non confined) liquid [1 7]. Several methods, such as mercury porosimetry, B.J.H. method, electron microscopy, Small Angle X-ray Scattering (SAXS), have been used for determining the pore size distribution of permeation polymer membranes and porous glass. Brun [2] gave the fundamentals of thermoporosimetry, a method which permits the determination of the pore size distribution as well as the shape of pores.

One of the major problems in DSC (Differential Scanning Calorimetry) experiments is the correspondence between the time and the true temperature of the sample during the scan. This correspondence is dependent on the mass of the sample, the thermal conductivity of the material and the thermal contact of the sample with the DSC pan. These thermal effects tend to shift and widen the DSC

* Author to whom all correspondence should be addressed.

1418–2874/98/ $ 5.00

Akadémiai Kiadó, Budapest
Kluwer Academic Publishers, Dordrecht

peaks and therefore affect the pore size distribution derived from the curves. If we want to have information of the pore size distribution, the scan rate V must be very slow. According to Brun, thermoporosimetry gives valuable results only if the scan rate V is lower than 0.1°C min^{-1}. But is this case the signal, which is proportional to V, is very weak and therefore the method is not accurate and thus useless. The aim of this paper is to show that by DSC measurements and thermoporosimetry it is possible to measure accurately the pore size distribution if a fractional method is used.

Experimental

The material used in this work is the butyl rubber type II characterized in [4]. Such composite materials serve as model systems for the investigation of the properties of confined water [4, 5]. Butyl rubber absorbs a certain amount of water despite the hydrophobic character of the chains. This is due to the nature and the amounts of fillers, cross-linking agent and chain ends, which may have hydrophilic character. These materials are used as linings to act against corrosion, and despite their hydrophobic character it has been demonstrated that water can migrate and form small droplets with size of the order of 10 to 30 Å as estimated by SAXS [4]. Other methods such as mercury porosimetry and B.J.H. method are not applicable.

The water uptake properties of butyl rubber depend on the mass fraction of the hydrophilic components [4, 5]. Two samples of type II (a and b) have been studied. In this work both materials have reached their swelling equilibrium. The swelling ratio S, ($S=m_w/m_0$, m_w being the mass of the absorbed water and m_0 the mass of the dry sample) is 0.16 and 0.06 for types a and b, respectively.

Typical DSC curves of a swollen sample, obtained with a Mettler DSC 30 instrument at different cooling and heating rates are given in Fig. 1a. The shape (in particular the peak width and intensity) of the curves changes with the scan rate, V. The glass temperature, T_g, of the different rubbers is located at −66°C (measured at 5°C min^{-1}). T_g does not depend on the concentration of water, this confirms that water is only present as droplets, since no plastification effect is observed.

The temperatures T_{on} and T_{off} corresponding to the beginning and end of melting, are indicated in the Figure. T_{on} does not depend on V and is only 1 or 2°C below the T_{on} value of ice for pure water. It is well known that the width $\Delta T=T_{off}-T_{on}$ of the melting peak of a pure compound increases with V and extrapolates to zero for $V=0$. This is not true in binary systems (polymer-water system [8] and in confined systems where a definite distribution of crystallite sizes exists [7]. In rubbers the width ΔT extrapolates to 2°C for $V=0$. It is clear then that the melting properties of ice (T_m and ΔT) in these rubbers are not very different from those of ice in pure water. Therefore it may be concluded that the analysis of the melting peak in a DSC scan cannot give accurate information on the distribution of crystallite sizes.

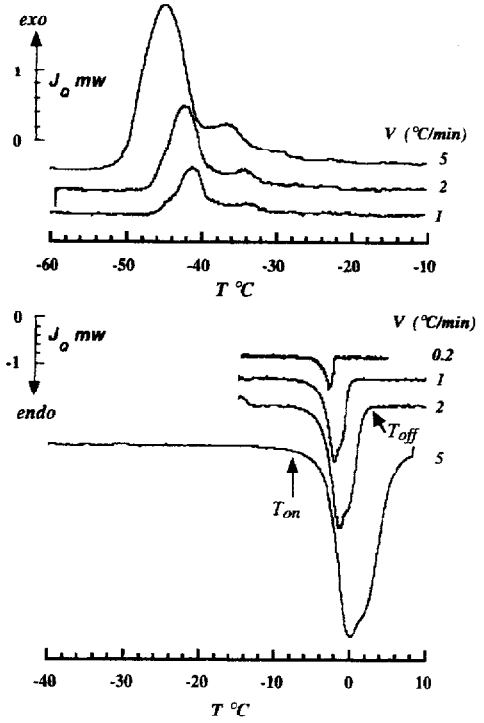

Fig. 1 DSC curves of butyl rubber IIa, swollen with water (S=0.16): endotherm and exotherm at different scanning rates V. The widths ΔT of the crystallization and melting peaks do not extrapolate to zero for V=0

The crystallization peak of ice exhibits similar features but it is important to note that the crystallization temperature T_c is very far from T_m and that the width of the exothermic peak, even if extrapolated to V=0 is much larger (10°C) than that of the endothermic melting peak. The difference between the shift of the crystallization temperature and the melting temperature of water in porous glass has been explained [2] by the difference in the curvature of a liquid-solid interface during the transformation process; during crystallization one can postulate that this interface always has a spherical shape (nuclei usually have this shape due to the surface energy) but during melting the shape of this interface has the form of the surface of the pores. This difference in the form of the solid–liquid interfaces could explain, via the Laplace pressure, the difference between the crystallization and melting temperature.

Fractionation method

The following method of fractionation is based on a series of isothermal crystallization (or melting) steps, followed by a classical DSC scan. During the first

step the material is in thermal equilibrium, it has partially crystallized (or melted) and during the second step the effect of annealing is revealed. Three types of thermal cycles are presented below to illustrate this fractionation method.

Fractionation of the crystallization peak: (Fig. 2a)

The swollen rubber is cooled rapidly to the annealing temperature T_a, in the crystallization domain, during a time t_a. In this domain the material crystallizes partially and an equilibrium is obtained by increasing the annealing time. The material is then heated to −8°C, at this temperature no melting occurs, then a DSC scan at a cooling rate of 5°C min^{-1} is done and the enthalpy $\Delta H(T_a)$ measured (due to the remaining amount of water which crystallizes during this last step). In a similar DSC scan but without previous annealing the total enthalpy of crystallization ΔH is obtained. The ratio $X_{C0}=(\Delta H - \Delta H_{(T_a)})/\Delta H$ is then the mass fraction of water which has crystallized at T_a. Figure 3a shows the fraction X_{C0}. It

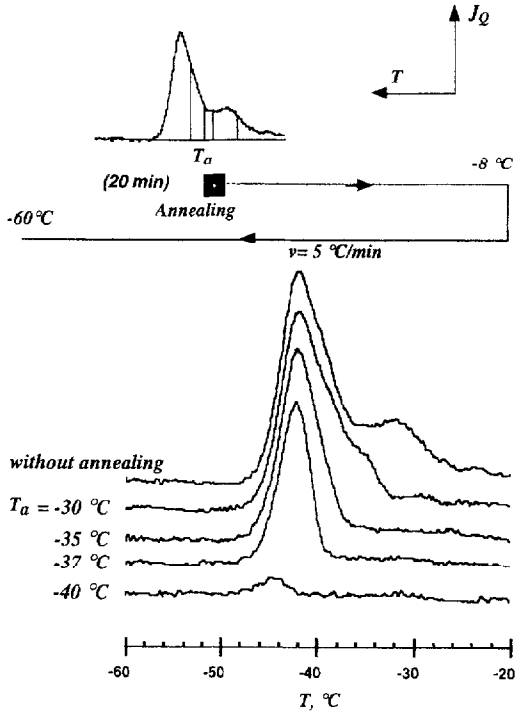

Fig. 2a DSC fractionation of the crystallization (a) and melting (b) peaks (see text) for swollen butyl rubber IIa (S=0.16). Method (a) involves three steps: an annealing in the crystallization domain at T_a, a rapid heating at −8°C well below the melting peak and then a DSC scan at 5°C min^{-1}; the exotherm curve is recorded during this last step

is important to note that this curve is the same for different annealing times (t_a=5', 20', 30'). Therefore it can be concluded that the crystallization of water in these rubbers is governed by thermodynamic and not kinetic factors. The derivative curve $X'_{C0}(T)$ gives then the true thermal curve (independent of the scanning rate). In the same figure are given the classical thermal curves X_{C5} and X'_{C5} obtained directly at 5°C min^{-1} without annealing; the comparison between the true curve $X'_{C0}(T)$ and the classical one X'_{C5} shows the importance of the kinetic effects during the DSC scan at 5°C min^{-1}. The exothermic peak is shifted by a few degrees (5°C) and the width of the true curve is about half of that observed in the classical method. In most published studies the scan rate is 10°C min^{-1} so in this case the difference would be even greater.

Fractionation of the melting peak: (Fig. 2b)

The same method is applied to the melting peak. All the water is crystallized first, and as before, the total enthalpy of crystallization, ΔH is measured. The material is

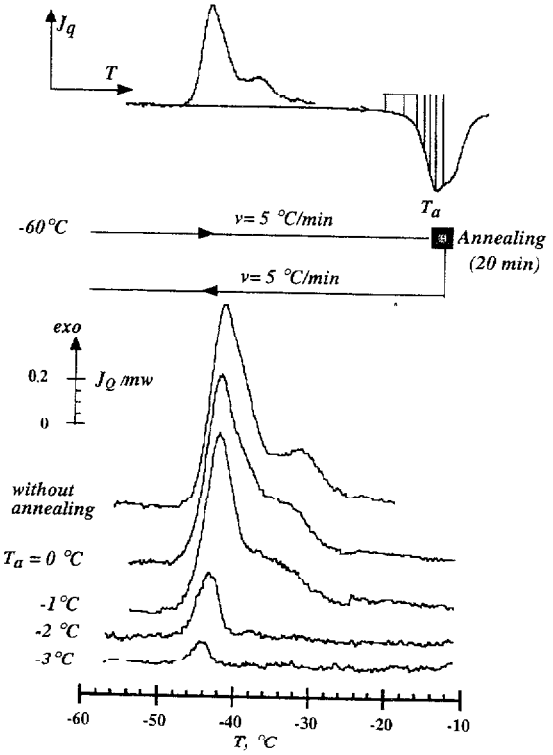

Fig. 2b DSC fractionation of the crystallization (a) and melting (b) peaks (see text) for swollen butyl rubber IIa (S=0.16). In method (b) water is crystallized completely at −60°C, the material is annealed at T_a in the domain of the melting peak of ice then the thermal curve is recorded during cooling at a rate of 5°C min^{-1}

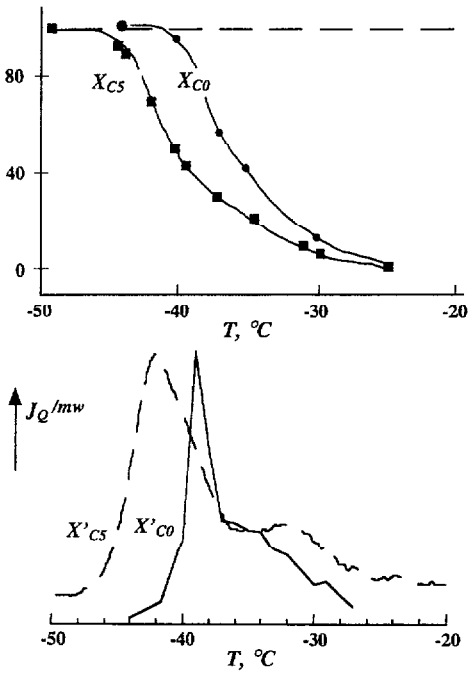

Fig. 3a By the fractionation method described in Fig. 2a the true integration curve X_{C0} (measured at V=0) is obtained. This curves gives the true fraction of water which has crystallized at the corresponding temperature. By discrete derivation of the X_{C0} curve one obtains the true crystallization curve X'_{C0}. These curves are compared to the direct curves X_{C5} and X'_{C5} obtained at a scanning rate of V=5°C min^{-1} (sample: butyl rubber IIa, S=0.16).

then annealed at T_a in the domain of melting (–3°C, 0°C). Annealing at –8, –5 and –3°C has no effect on the melting peak and are out of the real melting domain. The annealed material is then cooled at a constant rate of 5°C min^{-1} through the crystallization domain. The enthalpy measured ΔH_a corresponds to the water which was formed by the melting of ice at T_a. The fraction of water obtained by the melting of ice at T_a is $X_{m0}(T_a)=\Delta H_a/\Delta H$. It is important to note that the results obtained are again not dependent on the annealing time (for t_a>2 min). By derivation, this curve plotted in Fig. 3b gives the true melting curve. The most accurate curve is obviously $X'_{C0}(T)$ which has a width of about 10°C and not $X'_{m0}(T)$. The accuracy of the measurement is only limited by the regulation of the temperature of annealing (~0.2°C).

Fractionation of the crystallization peak by melting analysis

An equivalent method is described in Fig. 4a: the swollen sample IIb (S=0.06) is crystallized at T_a in the domain of crystallization (–25, –60°C) and then the thermal curve is recorded at a heating rate of 5°C min^{-1}. The enthalpy of melting

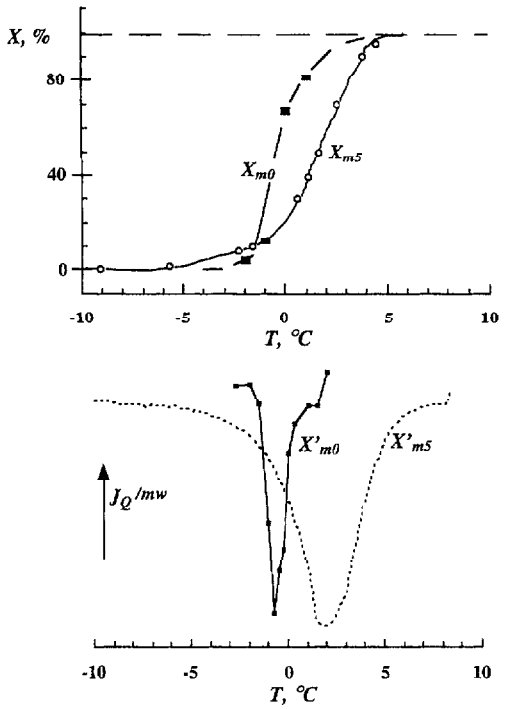

Fig. 3b By the DSC fractionation shown in Fig. 2b in a similar manner the integration curve X_{m0} giving the fraction of water which melts at the corresponding temperature is obtained and then the true curve X'_{m0}, for comparison, the DSC curve obtained in a classical way at 5°C min^{-1} is shown (sample butyl rubber IIa, C=13.8%)

$\Delta H_m(T_a)$ deduced from the melting peak is given in Fig. 4b which corresponds to the amount of water which crystallizes at temperature T_a; in the same Figure the derivative curve X' is compared to the DSC curve obtained at 5°C min^{-1}. It is clear that the fractionation method gives a true thermal curve without all the drawbacks of DSC (such as the effect of heating and cooling rates, thermal contacts and conductivity, etc.) since it was deduced from a succession of annealing steps. The interesting feature of this last method is that the melting peak for all the annealed samples appears in a narrow temperature range (−2 to −5°C), and the amount of ice melted is proportional to ΔH. No temperature correction of the melting enthalpy [2], as shown below, is necessary in this step.

Estimation of the pore size

Let us call x the fraction of water in droplets of radius greater than r

$$X(r) = \frac{m(r)}{m_{tot}} \tag{1}$$

$m(r)$ being the mass of water in the pores of size greater than r and m_{tot} the total mass of water in the sample. The pore size distribution is then given by dx/dr.

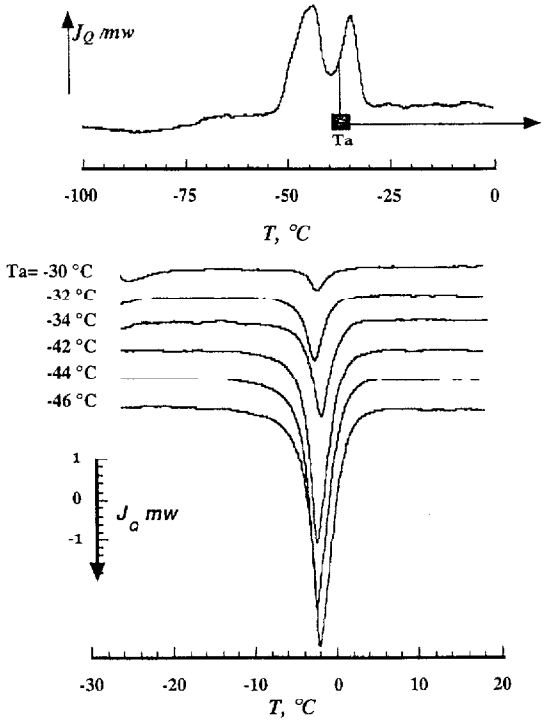

Fig. 4a Fractionation of butyl rubber IIb (C=6.25%) a) DSC curves at 5°C min^{-1} after annealing (crystallizing) the sample at T_a. The annealing time at T_a is 20 min

Now we apply thermoporosimetry as described by Brun *et al.* [2]. In order to have the droplet size distribution from a true thermal curve, we must have the relationship $r(\Delta T)$ between the pore size and the crystallization (or melting) temperature and the variation of the enthalpy with temperature. The Brun pore relationship between radius and the supercooling ΔT can be written as:

$$\Delta T = T_C - T_C^0 = -\frac{A}{r^*} \tag{2}$$

Two cases can be distinguished: a) r^* is the pore size when all water in droplets crystallized, b) r^* is a corrected value of the pore size, $r^*=r-0.57$ in nm, if we suppose that the first two layers of water at the solid interface do not crystallize; the theoretical value of A is 64.67 K nm^{-1} [2], the experimental value of A for water in porous alumina is 96 K nm^{-1} [1]. It must be pointed out that the Brun approach does not take into account the effect of supercooling due to nucleation (T_C^0 is then

0°C). In the same work this author shows that the enthalpy of crystallization (in J g^{-1}) of water is a function of the temperature of crystallization can be given as follows:

$$\Delta H(T) = -5.56 \cdot 10^{-2} \Delta T^2 - 7.43 \Delta T - 332 \quad (3)$$

A similar relationship was give n for the melting enthalpy [2]. We have to note that these relationships are only numerical approximations verified in the temperature domain $0<T<-50$°C.

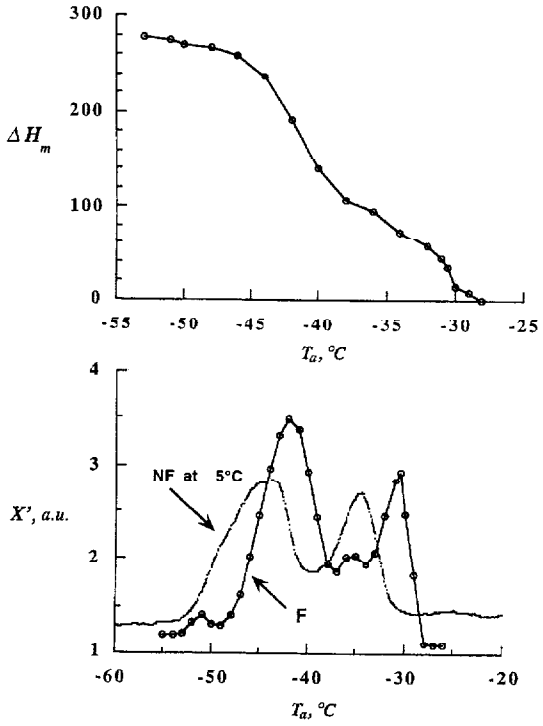

Fig. 4b Melting enthalpy ΔH_m and derivative curve $X'_{C0}=(d\Delta H)/(dT)$ as a function of the annealing (crystallization) temperature T_a. Comparison with curve X'_{C5} obtained at 5°C min^{-1} by the classical DSC method. The fractionation curve (F) contains more information that the classical curve (NF)

Using the relationship between the temperature and the pore size; the temperature scales of Fig. 3a and Fig. 4b are converted into a radius scale. The enthalpy corresponding to the crystallization of droplets between T and $T+dT$ is $X'_{C0}(T)dT$, then the fraction of droplets in which water crystallizes in this domain is given by:

$$dx = \frac{dTX'_{C0}(T)}{\Delta H(T)} \tag{4}$$

relations (2) and (4) give the pore size distribution:

$$\frac{dx}{dr} \approx \frac{\Delta T^2 X'_{C0}(T)}{\Delta H(T)}$$

This distribution is then normalized by the trapeze method. In Fig. 5a gives normalized pore size distribution deduced from the Brun relationships (2 and 3) and from the true thermal curve $X'_{C0}(T)$ of Fig. 4b obtained by the fractionation DSC method on sample IIa.

A bimodal distribution centred around 1.7 and 1.9 nm is obtained when it is assumed that there are no water layers at the interface which do not crystallize (curve α in Fig. 5a). This distribution is shifted to small sizes (curve β in Fig. 5a),

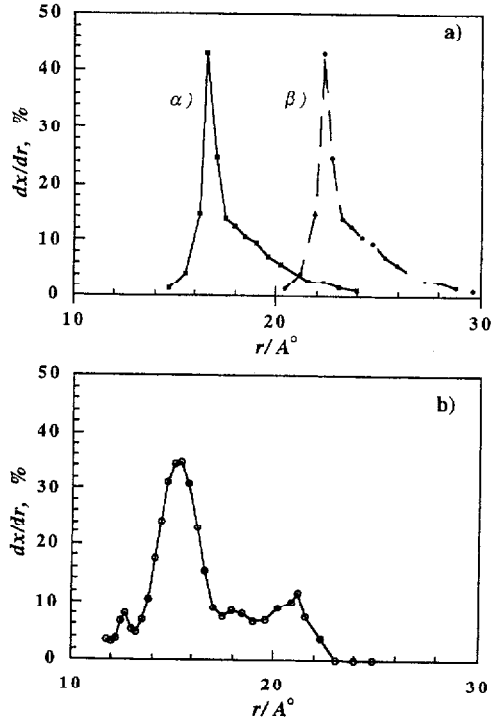

Fig. 5 The pore size distribution curve of water droplets in butyl rubbers deduced from the true crystallization curve and from relation (5). a) sample IIa of Fig. 3a; curve α corresponds to the case where all the water crystallizes in the droplets. Curve β corresponds to the case where a layer of two water molecules (0.57 nm thick) does not crystallize at the water/rubber interface. b) sample IIb of Fig. 4, all the water is supposed to crystallize, no non-crystalline interface layer between ice and rubber

if one assumes that a layer of 0.57 nm of water at the interface does not crystallize. These values are very close to those of Pelster *et al.* who used SAXS technique to study a similar butyl rubber. The important point is that the true width of this distribution Δr_1=0.2 and Δr_1=0.4 nm is obtained without special assumption on the form of the distribution as it is necessary in SAXS. At present the limited accuracy of DSC measurements, of the determination of water content and of the exact variation of the melting and crystallization enthalpy with the temperature do not permit any justified conclusion on the thickness of the interface layer of water which does not crystallize. Figure 5b shows the true pore size distribution of sample IIb deduced from the method described in Fig. 4a; as noted above, the important feature of this method is that no temperature correction (as used in Eq. (3)) is necessary because the melting temperature is nearly constant. It is clear that the distribution of pore sizes is not bimodal, this fractionation method discloses the presence of several types of pores (at least 4).

Similar distribution curves can be deduced from the fractionation experiments of the melting peak, but as indicated above with a much lower accuracy.

Conclusions

The different fractionation methods described above are only feasible when the domains of crystallization and melting of the solvent do not overlap. These methods permit to reconstruct true thermal curves which are independent of the scanning rate and independent of the amount of materials which undergo phase transition. These methods are appropriate for the study of concentrated and diluted solvent confined in different materials and which crystallize. Unlike SAXS experiments there are direct methods for studying the distribution of pore sizes in confined systems if one has a calibration method as in thermoporosimetry. These methods should be used to measure the confinement effect in polymer membranes with various concentration of crosslinks (PAA gels) and/or of crystallites (PVA etc). In such systems it is important to distinguish between the effect of confinement and of dilution [7, 8] on the properties of water.

* * *

This work was supported by the European INTAS 93-3379 program. We thank P. Pissis, R. Pelster, A. Kops and G. Nimtz for stimulating discussions and for preparation of the samples.

References

1 F. A. Dullien and V. K. Batra, Ind. Eng. Chem., 62 (1970) 25.
2 M. Brun, Thesis, Université Claude Bernard, Lyon, France 1973. M. Brun, A. Lallemand, J. F. Quinson and C. Eyraud, Thermochim. Acta, 21 (1977) 59. M. Brun, J. F. Quinson and L. Benoist, Thermochim. Acta, 49 (1981) 49.
3 Y. P. Handa, M. Zakrzewski and G. Fairbridge, J. Chem. Thermodyn., 18 (1986) 891.
4 R. Pelster, A. Kops, G. Nimtz, A. Enders, H. Kietzman, P. Pissis, A. Kryritsis and Woermann, J. Phys. Chem., 97 (1993) 666.

5 G. J. Briggs, D. C. Edward and E. B. Strorey, Rubber Chem. Technol., 376 (1963) 621.
6 G. Nimtz, A. Kops and R. Pelster in 'Hydrogen Bond Networks' edit. by M. C. Bellissent-Funel and J. C. Dore, NATO Series, 435 (1994) 419.
7 M. C. Bellissent-Funel, S. H. Chen and J. M. Zanotti, Phys. Rev., 51 (1995) 4558.
8 J. Rault, R. Grf, Z. Ping, Q. T. Nguyen and J. Neel, Polymer, 36 (1995) 1655.
9 T. Panomariova, Y. Melnichenko, P. A. Albouy and J. Rault, Polymer, 38 (1997) 3561.